LIMNOLOGY
and
OCEANOGRAPHY: METHODS

Limnol. Oceanogr.: Methods 6, 2008, 477–488

A microfluidic chemotaxis assay to study microbial behavior in diffusing nutrient patches

J.R. Seymour[1]*, *T. Ahmed*[1], *Marcos*[2], *R. Stocker*[1]

[1]Ralph M. Parsons Laboratory, Department of Civil and Environmental Engineering, Massachusetts Institute of Technology, 77 Massachusetts Ave, Cambridge, MA 02139 USA [2]Department of Mechanical Engineering, Massachusetts Institute of Technology, 77 Massachusetts Ave, Cambridge, MA 02139 USA

Abstract

The nutrient environment experienced by planktonic microorganisms is patchy at spatiotemporal scales commensurate with their motility (μm – cm), and the efficiency with which chemotactic microbes can exploit this heterogeneous seascape influences trophodynamics and nutrient cycling rates in aquatic environments. Yet, methodological limitations have largely prevented direct examinations of microbial behavior within heterogeneous microenvironments. We used soft lithography to fabricate a microfluidic-based chemotaxis assay to study the foraging response of aquatic microbes to diffusing microscale nutrient patches. The transparency, biocompatibility, and simplicity of microfluidic devices make them ideally suited for microbial ecology studies. A microinjector was used to create a 300 μm-wide nutrient band, simulating a pulse release of solutes. The chemotactic response of microbes to the diffusing patch was measured at the population and single-cell level. In contrast to traditional chemotaxis assays, this technique permits the assessment and quantification of chemotaxis toward a potential attractant in real time, enabling rapid screening of multiple chemicals. Furthermore, detailed information on chemotactic behavior can be obtained by tracking individual organisms. Here, we applied this microassay to study the chemotactic behavior of a range of aquatic microorganisms, including three marine bacterial isolates, a species of phagotrophic flagellate, and a species of phytoplankton. Each organism exhibited a rapid chemotactic response to a variety of chemical compounds, suggesting that many marine microbes are adapted to life within patchy microenvironments. The chemotaxis assay described here was found to be a flexible platform for studying both the specific case of microbes foraging within patchy habitats and as a broadly applicable tool for rapidly assessing and quantifying microbial chemotaxis.

Introduction

Chemotaxis is the directed movement of cells in response to chemical stimuli. Many eukaryotic and prokaryotic microorganisms are capable of orienting up or down chemical gradients by modifying swimming behavior (Eisenbach 2004), and diverse modes of chemotaxis have been identified among single-celled organisms (Kohidai et al. 1996; Eisenbach 1999; Fenchel and Blackburn 1999; Govoronova and Sineshchekov 2005; Mitchell and Kogure 2006). Bacteria represent the simplest and most-studied model for chemotaxis (Berg 2003). Bacteria propel themselves through liquid in nearly straight paths ('runs') by rotating helical flagella (Berg and Anderson 1973; Berg 1975), which are driven by proton and/or sodium-ion motors (Manson et al. 1977; Hirota and Imae 1983; Atsumi et al. 1992). They achieve speeds of tens to hundreds of micrometers per second. Directional changes occur when flagella rotation is reversed, typically causing either a 'tumble,' generating a random reorientation, or a reversal of direction, ultimately leading to a diffusive transport through the environment that has the statistical properties of a random walk (Berg 1975, 1993, 2003). Surface-bound chemotactic receptors allow bacteria to measure solute concentrations (Adler 1969) and modulate run lengths according to measured temporal concentration gradients. The resultant biased random walk drives a net migration of cells up a nutrient gradient or down a repellent gradient (Berg and Brown 1972; Brown and Berg 1974; Macnab and Koshland 1972), enhancing fitness within heterogeneous environments.

*Corresponding author: E-mail: justins@mit.edu

Acknowledgments

We are grateful to D. Hunt, M. Polz, and R. Belas for providing bacterial isolates, S. Stransky and T. Clay for the implementation of BacTrack, and three anonymous referees for insightful comments on the manuscript. This research was funded by NSF grant OCE-0526241. TA acknowledges support from a Martin Fellowship for Sustainability.

Bacterial chemotaxis first was observed over a century ago (Pfeffer 1888), and has since been studied widely and demonstrated to be a ubiquitous adaptation among a broad range of species. Several techniques have been developed to assess chemotaxis. The most frequently used is the capillary assay technique (Pfeffer 1888; modified by Adler 1969), based on immersing a capillary tube filled with a potential attractant (or repellent) into a suspension of bacteria and enumerating the cells that migrate into the capillary after a prescribed time. Other chemotaxis assays include swarm plates (Adler 1966), stop-flow diffusion chambers (Ford et al. 1991; Ford and Lauffenburger 1991), and cell tethering assays (Silverman and Simon 1974). However, most techniques are either organism-specific, time-consuming, or do not allow direct observation of behavior.

Due to the myriad of environments inhabited by microorganisms (Fenchel 2003), the ecological relevance of a chemotaxis assay depends on the phenotypic characteristics of the specific organisms and the physicochemical nature of their natural habitat. For instance, aquatic microbes often experience a heterogeneous and nutrient-deprived environment, characterized by sporadic and ephemeral microscale (μm – cm) patches of nutrients generated from several sources including the lysis of cells (Blackburn et al. 1997, 1998), excretions and exudations from other organisms (Lehman and Scavia 1982; Azam and Ammerman 1984; Mitchell et al. 1985), and leakage of substrates from sinking organic particles (Kiørboe and Jackson 2001). Hence, at sub-centimeter scales, the ocean is characterized by marked nutrient heterogeneity and the chemotactic foraging behavior of planktonic bacteria potentially can provide significant advantage in nutrient uptake (Blackburn et al. 1998; Kiørboe and Jackson 2001; Fenchel 2002; Stocker et al. 2008). Importantly, the typical life span of these microscale nutrient patches will be limited by the erosive effects of diffusion, so obtaining metabolic gains from a patch then becomes a race against time (Blackburn et al. 1997, 1998; Blackburn and Fenchel 1999*a*; Stocker et al. 2008). An understanding of marine microbial behavior within this dynamic and patchy nutrient landscape is important because efficient exploitation of nutrient patches by motile bacteria could have profound consequences for biogeochemical transformation rates (Azam 1998; Fenchel 2002). However, observations of microbial chemotactic foraging in patchy habitats have been hampered by methodological limitations and our current perception of these processes is based mostly on theoretical assumptions (Mitchell et al. 1985), numerical modeling (Bowen et al. 1993; Blackburn et al. 1997; Kiørboe and Jackson 2001), and evidence of bacteria clustering around randomly occurring and uncharacterized nutrient sources (Blackburn et al. 1998).

Recent advances in microfabrication techniques (Whitesides et al. 2001) and the application of microfluidic systems to study microbial ecology have opened new doors for studying behavior of microorganisms at environmentally relevant spatiotemporal scales (Park et al. 2003; Keymer et al. 2006; Marcos and Stocker 2006; Weibel et al. 2007; Stocker et al. 2008). Microfluidic devices consist of small chips onto which complex patterns, including microchannels, can be constructed accurately with micrometer precision (Whitesides et al. 2001; Weibel et al. 2007). Microfluidic chemotaxis assays have been proposed recently as sensitive and convenient alternatives to traditional assays (Mao et al. 2003; Diao et al. 2006; Koyama et al. 2006; Cheng et al. 2007). Here, we describe the design, fabrication, and application of a novel microfluidic chemotaxis assay, designed specifically for creating microscale nutrient pulses with dimensions and diffusive characteristics matching those predicted to occur in the ocean. We demonstrate how this device can serve both as a rapid and flexible qualitative chemotaxis assay with broad applicability to aquatic microorganisms, and as an effective quantitative platform for studying their behavioral responses to ephemeral resource patches.

Methods

Microchannel design—A microfluidic channel was designed and fabricated with the objective of creating a diffusing band of chemoattractant, to simulate an ephemeral, microscale nutrient patch. The microfluidic device was designed using AutoCAD software (Autodesk). The device consisted of a 45 mm long, 3 mm wide, and 50 μm deep channel (Fig. 1a). Two in-line inlet ports were used to introduce organisms (inlet *A*) and chemoattractants (inlet *B*) into the channel separately. Inlet *B* led to a 100 μm wide microinjector, which produced a coherent band of chemoattractants in the center of the channel (Fig. 1b).

Microfabrication—The microfluidic channel was fabricated using soft lithographic techniques (Whitesides et al. 2001). The channel design first was printed onto transparency film using a high-resolution image setter (Fineline Imaging) to create a 'design mask'. A negative photoresist, SU8-2050 (Microchem), was evenly spin-coated at 3000 rpm over the surface of a 4-inch silicon wafer to a thickness of 50 μm. The wafer was baked on a hotplate for 3 min at 65°C and then 6 min at 95°C. The design mask then was carefully placed face down on top of the silicon wafer and exposed to ultraviolet (UV) light at 3.5 mW cm^{-2} for 1 min using a Karl Suss MJB3 Mask Aligner (SPEC). Exposure to UV light polymerized exposed regions of the photoresist, appending a three-dimensional impression of the channel design onto the silicon wafer. The wafer was baked again at 65°C for 1 min and 95°C for 7 min, before being immersed in a developing agent (Polymonoacetate) for 2–3 min to remove the unexposed regions of the photoresist, rinsed with isopropanol to remove the developer, and blown dry with nitrogen.

Microchannels were fabricated out of the soft, silicon-based organic polymer—Polydimethylsiloxane (PDMS; Sylgard 184; Dow Corning). PDMS was mixed in a 10:1 ratio with its curing agent and poured over the developed wafer. The wafer

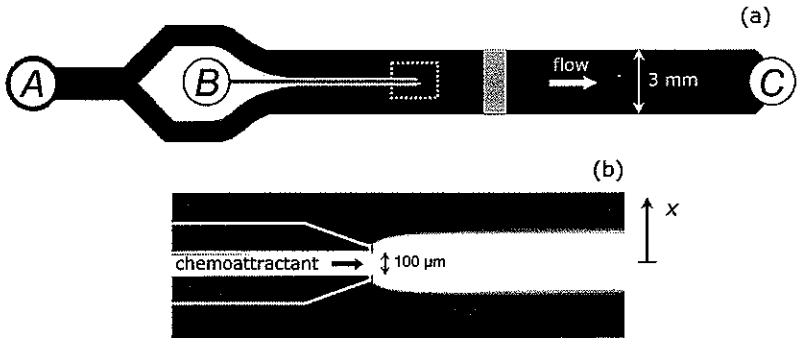

Fig. 1. The microfluidic chemotaxis assay. (a) Schematic of the microchannel (not to scale), showing the separate inlet points for organisms (*A*) and chemoattractants (*B*). The length and width of the channel are 45 and 3 mm, respectively. Data were collected 3 mm downstream of the microinjector tip, in the region shaded gray. Fluid leaves the channel via outlet *C*. (b) Epifluorescent image of the region in the dashed box in (a). Addition of 100 μM fluorescein enabled visualization of the chemoattractant band created by the microinjector. The outline of the microinjector's tip is overlaid for clarity.

then was oven baked at 65°C for 12 h, allowing the PDMS to set. The hardened PDMS, containing the channel structure, was cut using a razor blade and carefully peeled off the wafer. Holes for inlets and outlets to and from the microchannel were punched in the PDMS using a sharpened 16-gauge luer tip. The PDMS slab containing the microchannels was bonded to a glass microscope slide by exposing both to oxygen plasma for 1 min using a Plasma Cleaner/Sterilizer (Harrick Scientific). Following bonding, the channel was oven baked at 65°C for 10 min, rinsed with MilliQ water and stored at room temperature prior to use in experiments.

Experimental setup and procedure—The microfluidic channel was placed on the stage of an inverted microscope (Eclipse TE2000-E, Nikon). PEEK tubing (0.762 mm ID, 1.59 mm OD; Upchurch Scientific) was used to connect inlets A and B (Fig. 1) to 5 mL and 500 mL glass syringes (Hamilton), respectively. The outlet was connected to a constant-depth waste reservoir to prevent flow due to capillarity and gravity. Organisms and chemoattractants were injected simultaneously into the microchannel at a constant flow rate with a mean velocity of 240 μm s^{-1} using a syringe pump (PHD 2000, Harvard Apparatus).

To verify the formation of a coherent band of chemoattractant directly and monitor its subsequent evolution, fluorescent dye (fluorescein; Fluka) was added to chemoattractant solutions in a final concentration of 100 μM. The distribution of fluorescein was visualized by epifluorescence microscopy (Fig. 2a), using an EXFO X-Cite 120 fluorescent lamp (EXFO Photonic Solutions) and considered representative of the chemoattractant distribution, as the diffusivity of fluorescein is similar to that of low molecular-weight organic substrates. Organisms were observed at mid-depth in the channel, 3 mm downstream of the nutrient injection point (Fig. 1), using phase contrast microscopy and a long-working-distance 20 × objective.

After a stable band of chemoattractant had formed in the center of the channel (Fig. 2a), flow was stopped by turning off the syringe pump (time t = 0): this determined the start of the experiment. At this point, from the fixed point where

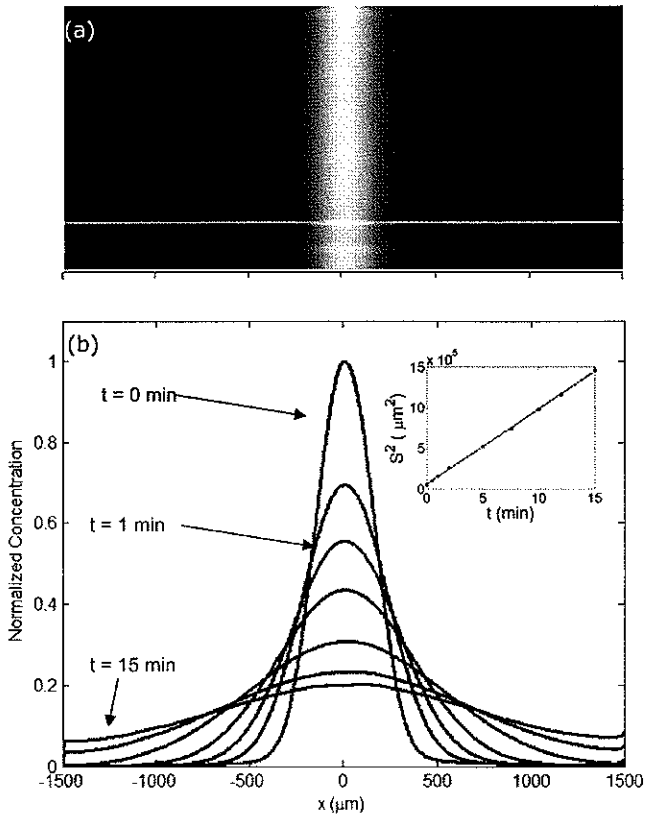

Fig. 2. Diffusion of the chemoattractant band. (a) Epifluorescent image of the band at $t = 0$. Similar images were obtained in real time at regular intervals during each experiment, providing a visual confirmation that the nutrient band was evolving smoothly as expected. (b) Evolution of the concentration profile across the microchannel over time. The curves correspond to $t = 0$, 0.5, 1, 2, 5, 10, 15, and 20 min, in decreasing order of maximum concentration. The position $x = 0$ is the center of the channel. Fluorescent intensities were normalized by the maximum intensity at $t = 0$. Inset: The square of the diffusion distance (S^2) increased linearly with time.

experiments were conducted, the chemoattractant band began to diffuse laterally. Due to the low Reynolds number of the flow in the channel (~0.01), all fluid motion stopped nearly instantaneously when the syringe pump was turned off, enabling the chemotactic response of microorganisms to be measured in flow-free conditions.

Data acquisition and processing—Distributions of organisms and fluorescent intensity across the microchannel were recorded at 1 min intervals for 10–15 min using a 1600 × 1200 pixel CCD camera (PCO 1600, Cooke) and variable magnification. At each point in time, a 'movie' (a sequence of 200–400 frames) was recorded at 10 or 32 frames per second (fps). Each frame was a 1600 × 1200 matrix of intensity (or 'gray') levels. By subtracting consecutive frames from one another, non-moving particles such as debris, non-motile cells, and dead cells were removed automatically from the analysis, allowing us to focus on motile cells and minimize noise levels. The microfluidic device enables one to assay the chemotactic response of swimming microbes at two levels of detail: (i) a real-time assessment of the occurrence and strength of chemotaxis, visualized and measured as accumulation of cells within the patch; and (ii) a quantitative analysis of single-cell chemotactic behavior, obtained by tracking trajectories of individual microorganisms.

In the first mode, the occurrence and relative strength of chemotaxis were assessed in two manners, both of them in real-time. First, image analysis software (IPlab, Scanalytics) was used to locate the maximum intensity value in each pixel across all frames in a movie – akin to a superposition of the frames or a long-time exposure photograph. We call this a cumulative trajectory plot. This plot gave an immediate visual representation of the cell distribution across the channel. Cell accumulation within the patch (i.e., the center of the channel) then was taken as an indication of chemotaxis. Second, we applied further image analysis to quantify the strength of chemotaxis. The position of all organisms within each frame was determined based on contrast with the image background ('segmentation'). After averaging over all frames, we could thus determine the distribution of cells across the channel (x direction). To express the strength of chemotactic accumulation relative to background levels, cell concentrations were normalized with respect to the mean concentration in the outermost 600 μm of the microchannel. To compare the strength of the chemotactic response between treatments readily using a single quantitative parameter, we computed a chemotactic index I_C, defined as the mean of the normalized cell concentration over the central 600 μm of the microchannel, corresponding to the position of the chemoattractant band.

In the second mode, information on the chemotactic behavior of single cells was obtained by reconstructing individual organisms' trajectories. This was performed using in-house developed cell-tracking Java software (BacTrack). Cell positions again were determined in each frame by segmentation, before linking positions among subsequent frames into trajectories using particle-tracking algorithms. The tracking process was performed *a posteriori*, due to the computational time required, which – although modest (2–10 min for a 400-frame movie on a Pentium M 1.73 GHz, depending on cell concentration) – prevented real time processing. Trajectories then were used to compute swimming statistics in Matlab (The MathWorks), including swimming speeds and turning frequencies. Swimming speeds were calculated from cell displacements between consecutive frames using center-differences. Turning frequencies were measured by defining turns operationally as changes in direction larger than 90°, which allowed for a relative comparison among different conditions for a given population.

Assessment

Nutrient patch generation—After exiting the microinjector, the band of chemoattractants immediately distended to an initial width of ~300 μm and formed a coherent band running the entire length of the channel (Fig. 2a). The initial width of this chemoattractant band can be set by adjusting the ratio of flow rates in inlets A and B (see below). At the point of measurement, the width of the band further depends on travel time from the microinjector's tip. Because diffusion begins as soon as the microinjector stream meets the main stream, a diffusion time equal to the distance of the measurement location from the microinjector tip (here, 3 mm) divided by mean flow speed (here, 240 μm s^{-1}) has elapsed when the flow is stopped. For our experiments, this time was 12.5 sec, resulting in a 570 μm wide band at the measurement location at time $t = 0$. When flow from both inlets was stopped, advection of organisms and chemoattractants ceased immediately and the chemoattractant band began to spread laterally at the measurement location (Fig. 2b), simulating a pulse release of nutrients. Visualization with fluorescein enabled us to track the concentration field over time. The width of the band reached ~2 mm after 5 min (Fig. 2b) and concentrations across the channel became homogeneous after ~30 min. The concentration in the central region of the channel dropped to < 20% of its original value after 15 min (Fig. 2b). The across-channel concentration of fluorescein, recorded across all pixels and averaged in the along-channel direction within the field of view, was least-square fitted to a 1D Gaussian profile using Matlab. Diffusion distance S varied with the square root of time, so the spatial variance of the Gaussian profile S^2 varied linearly with time (Fig. 2, inset). By fitting the theoretical prediction $S^2 = 2Dt$ to the data, the diffusion coefficient D of the band of fluorescein was found to be 7.7×10^{-6} $cm^2 s^{-1}$ (Fig. 2, inset).

Bacterial chemotaxis experiments—We applied the microfluidic chemotaxis assay to examine the chemotactic response of three marine bacterial isolates to various chemoattractants. Isolates of the marine bacteria *Pseudoalteromonas haloplanktis* (ATCC700530), *Vibrio alginolyticus* (12G01), and *Silicibacter sp.* (TM1040) were prepared according to specific growth requirements. All isolates were grown to mid-exponential growth

phase, at room temperature, while agitated on a shaker (175 rpm). *P. haloplanktis* was grown in 1% Tryptic Soy Broth (TSB; Difco) supplemented with NaCl [400 mM]. Cultures then were diluted 1:20 in an artificial seawater (ASW) solution (NaCl [400 mM], $CaCl_2.2H_2O$ [10 mM], KBr [1.7 mM], KCl [10 mM], $MgCl_2.6H_2O$ [20 mM], $MgSO_4.7H_2O$ [20 mM]), before being starved at room temperature for 72 h (modified from Mitchell et al. 1996). *V. alginolyticus* was grown in Vibrio Nine Salt Solution (VNSS) (Malmcrona-Friberg et al. 1990), centrifuged at 1,500 × g for 5 min and washed in Nine Salt Solution (NSS) (Malmcrona-Friberg et al. 1990). Silicibacter sp. (TM1040) was grown in half-strength 2216 marine broth (Miller et al. 2004), centrifuged at 1,500 × g for 5 min and washed in ASW. Prior to experiments, cell concentrations were diluted to 10^7 cells mL^{-1} in ASW or NSS, to optimize cell tracking.

We tested the response of the bacterial isolates to a variety of chemoattractants, including amino acids and phytoplankton extracellular exudates. L-serine and casamino acids (Fluka) were dissolved in ASW to final concentrations of 100 μM and 60 μg mL–1, respectively. The extracellular products ('exudates') of the marine phytoplankton species *Dunaliella tertiolecta* (CCMP1320), *Thallasiosira weissflogii* (CCMP1336), and *Synechococcus elongatus* (CCMP1630) were obtained from culture filtrates using the technique of Bell and Mitchell (1972). Axenic cultures of the three phytoplankton strains were grown to early exponential growth phase in sterile f/2 media (Guillard and Ryther 1962), supplemented with $Na_2SiO_3.9H_2O$ [11 μM] for *T. weissflogii*. Cells were centrifuged for 5 min at 500*g* and filtered through sterile 0.2 μm membrane filters (Millipore). The filtrate, containing the phytoplankton extracellular products, was employed as a chemoattractant for bacteria.

Assessing the chemotactic response of bacteria to microscale nutrient patches—The bacterial isolates exhibited varying levels of chemotactic response to the different chemoattractants. The nutrient band was initially devoid of bacteria, resulting in a gap in the bacterial concentration profile in the central region of the channel. Swimming cells rapidly (< < 1 min) filled this gap by random motility. Cells that were chemotactic toward the particular chemoattractant swam toward higher concentrations preferentially, resulting in the accumulation of cells within the central region of the microchannel. This accumulation was monitored in real time by the image processing software, which obtained movies directly from the camera and yielded a cumulative trajectory plot within seconds (Fig. 3a), as well as a histogram of cell distribution (Fig. 3b). This real-time processing enabled the detection of presence or absence of chemotaxis during the course of an experiment, along with an initial evaluation of its strength. Typically, a chemotactic response could be discerned in terms of cell clustering within several seconds from the start of the experiment, and always within < 5 min. The simplicity and rapidity of this semi-quantitative assessment enabled quick screening of the chemotactic response of a given organism to several different

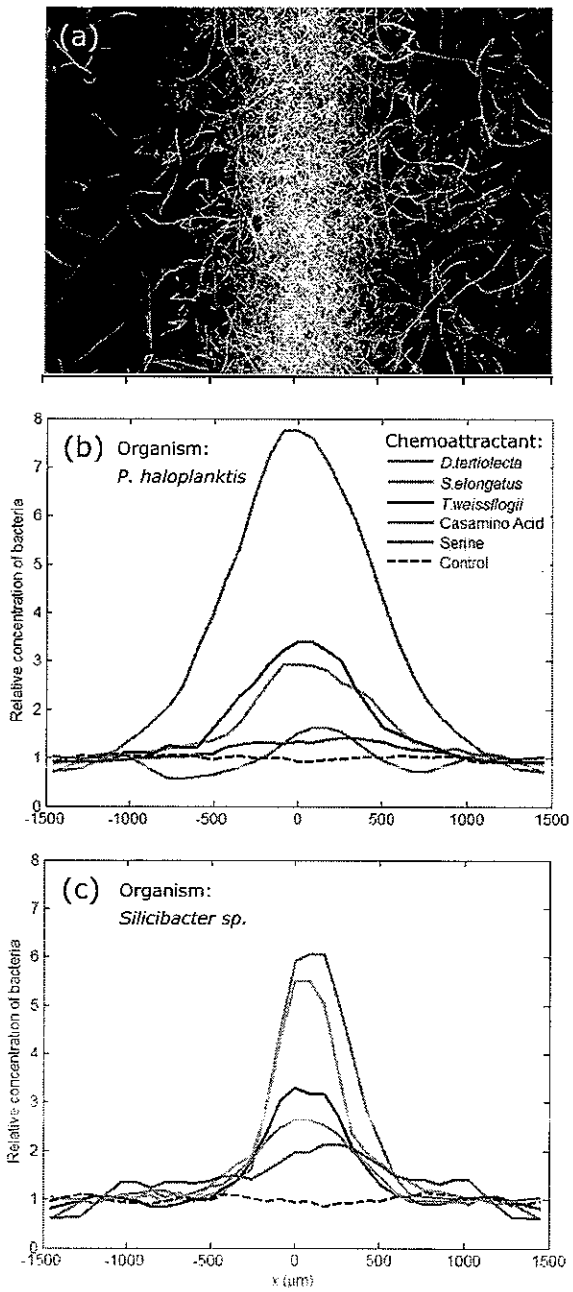

Fig. 3. Chemotactic accumulation of bacteria within bands of different chemoattractants. (a) Cumulative trajectory plot, obtained in real time and used to qualitatively assess the presence or absence of chemotaxis. Shown is a collection of trajectories of *P. haloplanktis* bacteria responding to a band of *D. tertiolecta* exudates. Each white path is a single trajectory: the accumulation indicates a strong chemotactic response. The image was obtained from a movie recorded at $t = 2$ min, over 12.5 s at 32 fps, and 100 × magnification. (b) Concentration of *P. haloplanktis* cells across the microchannel at $t = 5$ min for different chemoattractants. Bacterial concentrations were normalized with the mean bacterial concentration measured in the 600 μm closest to the edge of the microchannel. (c) As (b), for *Silicibacter* TM1040.

chemoattractants. For each strain of bacteria investigated here, all six chemoattractants were screened in < 2 h.

For the most potent attractants, intense aggregations of bacteria occurred inside the chemoattractant band within < 1 min. Clear accumulations of cells sometimes persisted for over 15 min, before returning to a uniform distribution as the chemoattractant became homogeneous across the channel. The strength of the chemotactic response, quantified here by the chemotactic index I_c, varied across chemoattractants and organisms (Table 1; Figs. 3, 4). The strongest response was exhibited by *V. alginolyticus* in response to the *D. tertiolecta* exudates, with $I_c = 7.35$. The most potent chemoattractants typically were the exudates of *D. tertiolecta* and *T. weissflogii* ($I_c \geq 3$), with the lowest levels of attraction (e.g., $I_c = 1.33$ for *P. haloplanktis*) typically observed for serine. The nature of the chemotactic accumulation also differed between treatments, with some chemoattractants triggering narrow and concentrated hot spots of bacteria (Fig. 3a) and others inducing broader and more disperse bands, likely due to differences in the chemotactic sensitivity of bacteria to different substrates. In some cases, secondary bands of bacteria formed on the edges of the concentration gradient, possibly indicative of a threshold response and chemoreceptor saturation. In control experiments where ASW or NSS, supplemented by 100 μM fluorescein, were injected into the channel, no accumulation of cells was observed.

Characterization of the bacterial behavioral response—A distinct feature of our setup is that the analysis of the chemotactic response can be taken to a more detailed level by using image analysis and cell tracking to quantify the swimming behavior of individual cells. Information on swimming statistics, such as speed and turning frequency, enables one to detect shifts in the swimming behavior induced by chemoattractants. Simultaneous knowledge of swimming statistics and chemoattractant concentration distribution makes it possible to relate behavioral changes to nutrient conditions, which is imperative for understanding both foraging behavior and chemotactic migration dynamics of populations. In these experiments, we detected significant shifts in swimming behavior, particularly for *P. haloplanktis*. In comparison to the control case consisting of a chemoattractant-free suspension, *P. haloplanktis* swam faster and increased turning frequency when exposed to a chemoattractant band (Fig. 5). This observation is consistent with previous observations for this species (Barbara and Mitchell 2003*a*,*b*; Seymour et al. 2008 in press). In the presence of a nutrient band, swimming speeds were higher inside the band than outside (Fig. 5a), indicative of a chemokinetic response, wherein nutrient stimuli lead to increased bacterial swimming speeds (Zhulin and Armitage 1993; Packer and Armitage 1994; D'Orsogna et al. 2003). After 2 min from the onset of the experiment, the turning fre-

Table 1. Chemotaxis index I_c for three bacterial isolates in response to different chemoattractants, measured at $t = 5$ min after release of the nutrient patch. The values of $I_c < 1$ in the control experiments reflect the fact that the initial void of bacteria in the center of the channel, corresponding to the initial position of the chemoattractant band, has yet to be completely filled by random bacterial motility at $t = 5$ min Differences in I_c between control cases for different isolates are due to differences in swimming speeds among isolates.

Chemoattractant	Bacterial Isolates		
	P. haloplanktis	*Silicibacter sp.*	*V. alginolyticus*
Control (ASW)	0.98	0.93	0.70
*D. tertiolecta**	7.26	5.06	7.35
*S. elongatus**	2.76	4.51	2.61
*T. weissflogii**	3.25	2.92	3.94
Casamino acids	1.41	2.52	2.80
Serine	1.33	1.91	4.53

*extracellular exudates of phytoplankton species obtained using the method of Bell and Mitchell (1972).

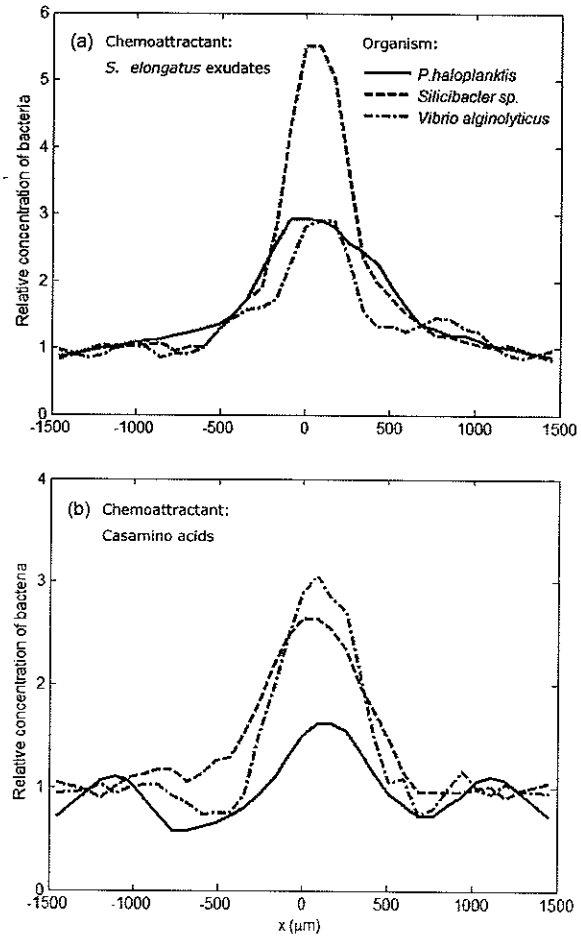

Fig. 4. Chemotactic accumulation of three bacterial isolates within bands of (a) *S. elongatus* extracellular products, and (b) casamino acids (60 μg mL^{-1}), at $t = 5$ min. Bacterial concentrations were normalized as in Fig. 3b.

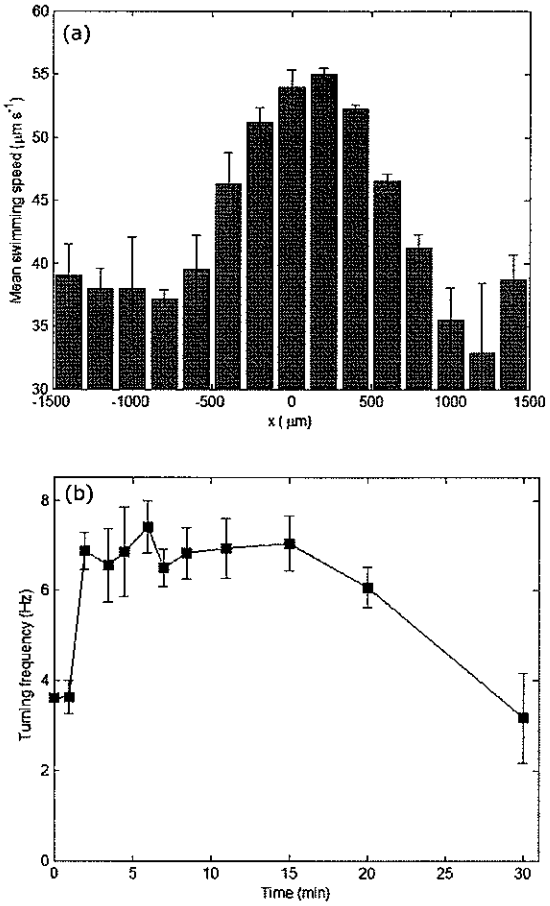

Fig. 5. (a) Distribution of mean swimming speed across the channel for *P. haloplanktis* bacteria exposed to a band of *S. elongatus* extracellular products, recorded at $t = 5$ min. The mean was computed over the number of bacteria in a given region and error bars are standard deviations (n ~ 10,000 bacteria). (b) Mean turning frequency of *P. haloplanktis* over time, following exposure to a band of *D. tertiolecta* extracellular products. Time $t = 0$ corresponds to the release of the patch, which occurred by stopping the flow in the channel. The mean was computed over all bacteria across the width of the channel and error bars are standard deviations.

quency of *P. haloplanktis* nearly doubled (Fig. 5b) and returned to its initial value after 30 min. Enhanced turning frequencies are in line with previous observations of *P. haloplanktis* (Barbara and Mitchell 2003*b*), but in contrast, for example, to *E. coli*, which reduces turning frequency when swimming up a gradient of chemoattractant. In control experiments with ASW and 100 μM fluorescein, *P. haloplanktis* showed no changes in swimming behavior, indicating that the shifts observed here were a direct behavioral responses to the band of chemoattractant.

Applicability to other organisms—To demonstrate the broad applicability of the microfluidic chemotaxis assay, we further tested it on aquatic eukaryotic microbes, including species of phytoplankton and heterotrophic flagellates. The response of swimming phytoplankton to bands of inorganic nutrients (NH_4^+) was measured in the same manner as above, using the swimming chlorophyte *D. tertiolecta* (CCMP1320). When exposed to bands composed of NH_4Cl (1 μM–1 mM), *D. tertiolecta* cells exhibited rapid chemotaxis, with strong accumulation of cells observed within 1–2 min (Fig. 6a,b), leading to an I_C value of 4.13. These results indicate that motile phytoplankton may experience elevated nutrient concentrations by exploiting microscale resource patches, such as those produced by zooplankton excretions (McCarthy and Goldman 1979).

We also examined the foraging response of the heterotrophic flagellate *Neobodo designis* (CCAP1951/1) to microscale patches of bacterial prey. For this case, the procedure described above was modified slightly, so that a band of prey (the bacteria *P. haloplanktis*) – rather than of chemoattractants – was injected into the channel via inlet *B*. The chemotactic foraging response of aquatic bacterivores has been studied previously by attaching bacteria to the surfaces of capillaries or embedding them within agar (Fenchel and Blackburn 1999). Our assay enables the visualization of phagotrophic organisms as they swim through suspended prey patches, a more realistic configuration to study the behavior of microbial predators in a patchy food habitat. In a control case, where bacteria-free TSB medium was injected into the channel, *N. designis* cells swam in relatively straight trajectories, with few changes in direction (Fig. 6c). However, when a band of bacterial prey was injected into the channel, a clear foraging response was observed. In line with our previous observations (Seymour et al. 2008 in press), we found that *N. designis* cells modified their swimming behavior by decreasing speed and increasing path tortuosity, allowing individual cells to maintain their positions within the bacterial band for several minutes (Fig. 6d), where they presumably exploited the elevated prey densities. In the environment, behavior of this kind can increase predation efficiency (Nachman 2006) and, ultimately, may accelerate the flux of carbon from the microbial loop further up the aquatic food web.

Discussion

In recent years, microfluidic devices have been applied successfully to create sub-millimeter scale chemical gradients (Jeon et al. 2000; Dertinger et al. 2001; Wu et al. 2006; Stocker et al. 2008) and as chemotaxis assays for various organisms (Mao et al. 2003; Diao et al. 2006; Koyama et al. 2006; Cheng et al. 2007; Ahmed and Stocker 2008 in press). Microfluidics presents several key advantages over previous chemotaxis assays. First, the accuracy of fabrication of a microchannel's architecture (< 5 μm) along with the laminar nature of the flow within microchannels allows fine-scale control and high reproducibility of flows and concentration gradients within volumes commensurate with the microenvironments of microbes. Consequently, more reliable gradients can be created compared to traditional macroscopic capillary assays, where gradients are difficult to quantify and easily perturbed

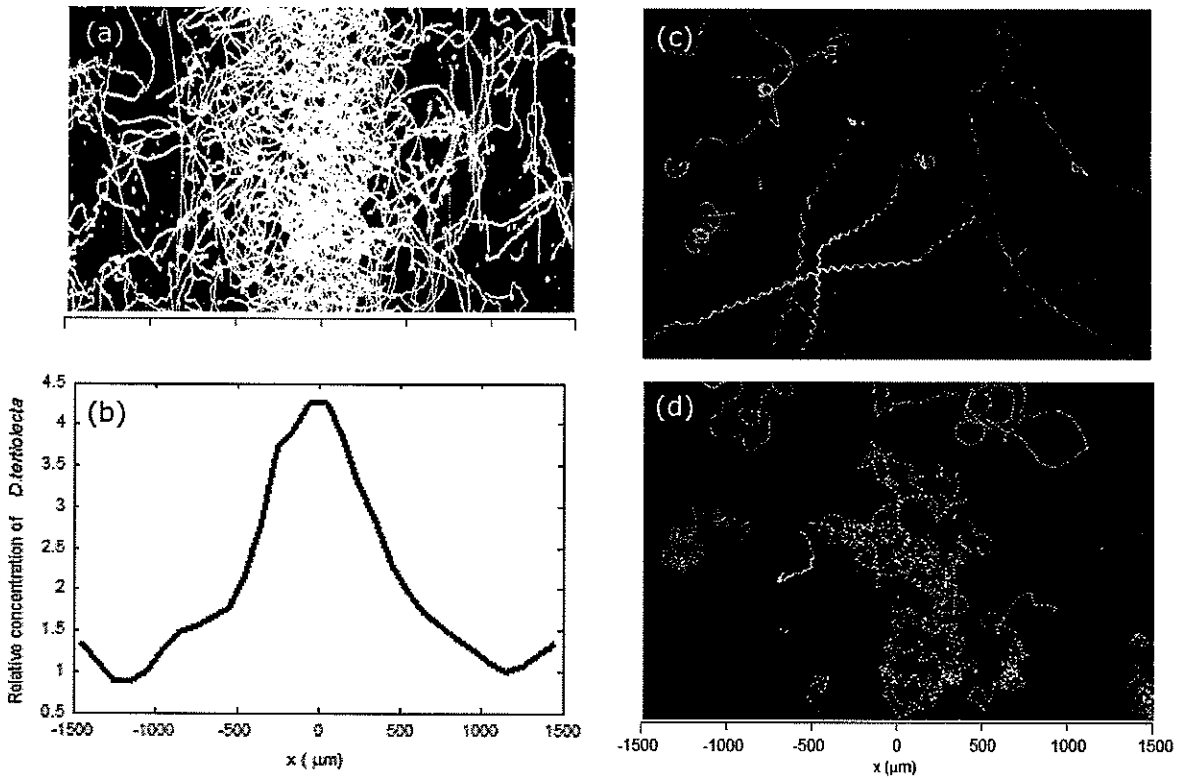

Fig. 6. Chemotactic response of marine eukaryotic microbes. (a) Trajectories of the phytoplankton *D. tertiolecta* accumulating in a band of 100 μM NH_4^+ (b) Distribution of *D. tertiolecta* cells across the channel width after exposure to a band of 100 μM NH_4^+. Cell concentrations were normalized as in Fig. 3b. (c,d) Trajectories of the flagellate *N. designis* in the absence of prey (c) and in response to a band of bacterial prey (*P. haloplanktis*) injected into the microchannel in lieu of a chemoattractant (d). Note the accumulation in the central region as well as the strong increase in path tortuosity in (d), compared to (c). For all panels, trajectories were obtained from a movie recorded over 40 s at 10 fps and 40 × magnification.

by even minor residual flows (Vicker 1981). Second, the transparency of the PDMS-based microchannels is ideal for microscopic visualization, enabling real-time assessment of the presence or absence of a chemotactic response, as well as cell-tracking and detailed post-processing of swimming statistics. This flexibility is unprecedented in chemotaxis assays and ideally suited for studies in aquatic microbial ecology.

Previous microfluidic chemotaxis assays can be classified broadly as flow-based or static systems. The former exploit flow to create a constant chemical gradient across streamlines in a laminar flow (e.g., Mao et al. 2003; Koyama et al. 2006; Lin and Butcher 2006). This establishes a steady gradient at a given channel location, yet the gradient experienced by organisms varies over time because they are transported through the channel. Furthermore, flow complicates the detailed analysis of swimming behavior, because it is impossible to eliminate hydrodynamic influences on the movement of cells. The alternative, static gradient systems are advantageous in this respect, as they can be used to generate gradients that remain constant over time in the absence of flow, by allowing chemicals to diffuse across a permeable membrane or hydrogel from an adjacent reservoir of chemoattractant (Diao et al. 2006; Wu et al. 2006; Cheng et al. 2007). However, as gradients are established by diffusion, these techniques typically require significant time to assess chemotaxis, preventing rapid screening of multiple chemoattractants. Furthermore, neither method is appropriate for investigating chemotactic responses to an ephemeral diffusing nutrient pulse under flow-free conditions. The device presented here is a hybrid of the two categories described above, as flow is used to establish a chemical gradient rapidly, and chemotaxis subsequently occurs in the absence of flow. In this respect, our method is similar to stopped-flow diffusion assays (Ford et al. 1991; Lewus and Ford 2001). It differs from those, however, in two main respects. First, the microinjector enables the generation of a nutrient patch of a given size, reproducing the competition between the time scales of patch diffusion and bacterial chemotaxis predicted to occur in aquatic environments (Blackburn et al. 1997, 1998; Stocker et al. 2008). Second, the integration with videomicroscopy as opposed to the use of light-scattering techniques (Ford et al. 1991; Lewus and Ford 2001) allows for quantification of behavioral mechanisms associated with chemotaxis by measuring the positions and trajectories of single cells.

The device described here was designed with the specific purpose of measuring the strength and speed of the chemotactic response of marine microorganisms to a diffusing patch of nutrients. The lifetime of the chemoattractant band is comparable to that of microscale nutrient patches predicted to occur in the ocean (~10 min) (Lehman and Scavia 1982; Blackburn et al. 1997; Kiørboe and Jackson 2001). The predicted dimensions of short-lived pulses of dissolved nutrients in the ocean (Lehman and Scavia 1982; Mitchell et al. 1985; Blackburn et al. 1997, 1998) typically are below the Kolmogorov length scale (Lazier and Mann 1989), hence, turbulent dispersion is negligible and patches spread primarily through diffusion (Blackburn et al. 1997; Blackburn and Fenchel 1999*a*). The initial width of the chemoattractant band (~570 μm) was comparable to the size of a nutrient patch produced by a zooplankton excretion event (Jackson 1980; Lehman and Scavia 1982) or the DOM plume associated with a marine snow particle (Kiørboe and Jackson 2001). Nutrient patches in the ocean can be generated by numerous processes, and may range in size from several centimeters (Seuront et al. 2002) down to a few micrometers, such as may occur following the lysis of a small phytoplankton cell. Different sized patches can be investigated with our device by simply tuning the relative flow rate in the two inlets to compress or broaden the chemoattractant band upon release from the microinjector. To demonstrate this versatility, we conducted an experiment using two separate syringe pumps to control the flow rates Q_1 and Q_2 differentially at inlets *A* and *B*, respectively. Volume conservation then predicts the width of the band to be $WQ_2/(Q_1 + Q_2)$, for a given microchannel width *W*. Experimental measurements verified that the width of the band closely followed this theoretical relation (Fig. 7), confirming applicability to mimic patches of variable size, from ~10 μm to ~1 mm.

Using this microfluidic chemotaxis assay, we observed strong chemotactic responses by marine bacteria to various attractants. Bacteria displayed intense aggregations, often reaching several times background levels. Furthermore, the microfluidic assay allowed us to determine the rates at which bacteria home in on nutrient patches, with strong accumulations of cells occurring within < 1 min and persisting for 10–20 min. These observations confirm that some marine bacteria can exhibit very rapid chemotactic responses to exploit diffusing nutrient patches and obtain 10–15 min bursts of elevated nutrient concentrations. The collection of cell distribution data affords great flexibility in the quantification of chemotaxis. Here we were concerned with the formation of bacterial 'hot-spots' and defined a chemotactic index I_C. However, alternative metrics can be implemented easily, for example to measure relative nutrient gain by correlating distribution of cells and nutrients (Stocker et al. 2008).

Marine bacteria inhabit a world quite dissimilar to that experienced by other bacteria, and their swimming and chemotactic behaviors consequently may differ markedly from *E. coli*, the model for bacterial chemotaxis (Berg 1993; Barbara and Mitchell 2003*a*,*b*; Mitchell and Kogure 2006). Current understanding of the swimming strategies of marine bacteria is severely limited, however, and most theoretical models of bacterial chemotaxis in the ocean necessarily, but perhaps erroneously, apply parameters measured for *E. coli* (e.g., Jackson 1987, 1989; Bowen et al. 1993). Using this assay we have shown, both here and elsewhere (Seymour et al. 2008 in press), that some marine bacteria significantly increase swimming speed and turning frequency when exposed to microscale nutrient patches. These behavioral shifts contrast with the typical chemotactic behavior of *E. coli*, and should be taken into account to better model the role of marine bacteria in ocean nutrient cycles. A point of caution when using microfluidic devices is that swimming patterns can be affected by the vicinity of a solid surface (DiLuzio et al. 2005; Lauga et al. 2006; Hill et al. 2007). This effect occurs within a few body lengths (< 10 μm; Frymier et al. 1995) from surfaces, and is thus minimized by making observations at mid-depth of a > 50 μm-deep channel.

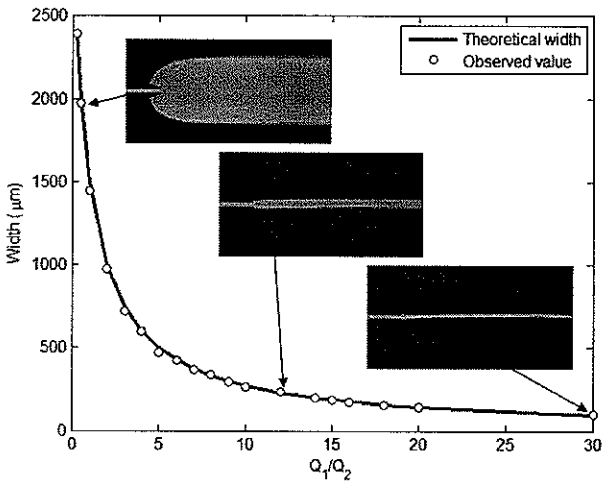

Fig. 7. Width of the nutrient band as a function of the ratio of flow rates between inlet *A* (flow rate Q_1) and *B* (flow rate Q_2). The solid line represents the width $WQ_2/(Q_1 + Q_2)$ predicted from volume conservation, where $W = 3$ mm is the microchannel width. The circles are experimental observations obtained by varying Q_1 from 125 to 15000 mL/hr, while Q_2 was fixed at 500 ml/hr. The three insets show epifluorescent images of the nutrient band visualized using fluorescein for $Q_1/Q_2 = 2$, 12 and 30.

We have demonstrated that this microfluidic chemotaxis assay is applicable to a wide range of microorganisms. In addition to marine bacteria, we have applied it to other bacteria including *Helicobacter pylori* and *E. coli*, and to phagotrophic predatory organisms feeding on aggregations of prey cells. We currently are pursuing the differential labeling of cells to simultaneously track predators and prey or competing microbial populations. The primary limitation on the range of aquatic organisms that can be studied is set by the depth of the device: application to larger organisms such as dinoflagellates or most zooplankton would require fabrication of channels

deeper than the 50 μm used here. We previously have achieved channel depths of up to 500 μm using the same fabrication techniques.

Although this microfluidic device was developed originally to study the specific scenario of aquatic microbes foraging in a patchy resource habitat, we have since found that it also is a rapid and informative chemotaxis assay, as it allows for immediate observation of cell accumulation within a chemoattractant band. Both the absolute chemoattractant concentration and the shape or intensity of concentration gradients are expected to determine a microbes' chemotactic response, and both can be measured directly in this setup. In contrast to traditional chemotaxis assays that rely on plating of bacteria to quantify chemotaxis, thus requiring many hours or days and introducing considerable uncertainty in the results, our technique yields a first estimate of the occurrence and strength of chemotaxis in real time. This system has proven to be extremely useful in our laboratory when rapid screening for chemotaxis of an organism toward potential chemoattractants is required. The short time frames for individual experiments allow relatively high-throughput comparative studies. Parallelization and use of valving systems (e.g., Quake and Scherer 2000; Unger et al. 2000) could be used to further increase throughput, but we have opted for simplicity, achieving ~ 4-6 runs h^{-1}. Furthermore, one can achieve high levels of replication, often not feasible in other, more time-consuming chemotactic assays, potentially providing new information on the noise associated with the chemotactic response of microorganisms (Korobkova et al. 2004).

It is becoming increasingly evident that distributions of organic matter and microorganisms in aquatic systems are patchy at scales commensurate with the locomotory abilities and sensory perceptions of individual cells (Fenchel 2002; Azam and Malfatti 2007). At the same time, behavioral responses to chemical signals appear to be ubiquitous features within the microbial food web, with diverse organisms responding differently to a wide range of chemical compounds (Seymour et al. 2008 in press). Beginning to unravel this complex web of interactions hinges partly on the availability of simple and rapid tools to assess microbial behavior within patchy resource landscapes. We believe that devices based on microfluidic technology and image analysis, like the one presented here, hold great promise in this respect and we expect microfluidic technology to deepen understanding of the ecology and trophic interactions at the ocean's microscale.

Comments and recommendations

We have shown that two complementary modes of analysis are possible: (i) real-time, population-scale data, potentially allowing one to determine chemotactic migration rates, dissociation constants, chemotactic sensitivities, and random motility coefficients (Berg and Brown 1972; Mesibov et al. 1973; Brown and Berg 1974; Lovely and Dahlquist 1975); and (ii) single-cell data, to obtain information on the chemotactic behavior including swimming speeds, run durations, run lengths, and turning angles. A further advantage of this technique is the unprecedented ability to measure spatiotemporal distributions of concentrations simultaneously with bacterial distributions and trajectories, enabling one to correlate bacterial distribution or swimming statistics with the concentration field (Seymour et al. 2008 in press) or estimate increases in nutrient exposure experienced by chemotactic cells (Stocker et al. 2008).

The facilities required for experiments of the type described here can be divided into two categories. First, microfabrication tools and facilities are required. These are becoming increasingly available at research institutions, often as shared cleanroom facilities. Alternatively, microchannels can be fabricated for the user without the need for specialized skills on the user's behalf by commercial foundries (e.g., the Stanford Microfluidics Foundry http://thebigone.stanford.edu/foundry). Second, the equipment to perform the actual chemotaxis experiments is needed. This includes a microscope (preferably inverted) with epifluorescent illumination, a digital video-camera and image analysis software, and a syringe pump. Although great flexibility is available in image-processing software, we found the capability of processing movies in real time an essential feature of our setup. A variety of microscopy software (e.g., IPLab; Metamorph) can provide this functionality.

Ultimately, the rapid ongoing developments in the field of microfluidics will pave the way for further improvements in the ability to perform manipulative experiments in microbial ecology. Assimilating these novel techniques and adding them to the toolbox of limnologists and oceanographers will prove extremely valuable for studying microbial ecology at the smallest scales.

References

Adler, J. 1966. Chemotaxis in bacteria. Science 153:708–716.

———. 1969. Chemoreceptors in bacteria. Science 166:1588–1597.

Ahmed, T., and Stocker, R. 2008. Experimental verification of the behavioral basis of bacterial transport parameters using microfluidics. Biophys J. In press.

Atsumi, T., L. McCarter, and Y. Imae. 1992. Polar and lateral flagellar motors of marine *Vibrio* are driven by different ion-motive forces. Nature 355:182–184.

Azam, F. 1998. Microbial control of oceanic carbon flux: The plot thickens. Science 280:694–696.

———, and J. W. Ammerman. 1984. Cycling of organic matter by bacterioplankton in pelagic marine ecosystems: Microenvironmental considerations, p. 345–360. *In* M. J. R. Fasham [ed.] Flows of energy and materials in marine ecosystems. Plenum Press.

Azam, F., and F. Malfatti. 2007. Microbial structuring of marine ecosystems. Nature Rev. Microbiol. 5:782–791.

Barbara, G. M., and J. G. Mitchell. 2003*a*. Marine bacterial organisation around point-like sources of amino acids. FEMS Microbiol. Ecol. 43:99–109.

———, and J. G. Mitchell. 2003*b*. Bacterial tracking of motile algae. FEMS Microbiol. Ecol. 44:79–87.

Bell, W., and R. Mitchell. 1972. Chemotactic and growth responses of marine bacteria to algal extracellular products. Biol. Bull. 143:265–277.

Berg, H. C. 1975. Bacterial behaviour. Nature 254:389–392.

———. 1993. Random walks in biology. Princeton University Press.

———. 2003. *E. coli* in motion. Springer.

———, and R. A. Anderson. 1973. Bacteria swim by rotating their flagellar filaments. Nature 245:380–382.

———, and D. A. Brown. 1972. Chemotaxis in *Escherichia coli* analysed by three-dimensional tracking. Nature 239:500–504.

Blackburn, N., F. Azam, and Å. Hagström. 1997. Spatially explicit simulations of a microbial food web. Limnol. Oceanogr. 42:613–622.

———, and T. Fenchel. 1999*a*. Influence of bacteria, diffusion and shear on micro-scale nutrient patches, and implications for bacterial chemotaxis. Mar. Ecol. Prog. Ser. 189:1–7.

———, T. Fenchel, and J. G. Mitchell. 1998. Microscale nutrient patches in plankton habitats shown by chemotactic bacteria. Science 282:2254–2256.

Bowen, J. D., K. D. Stolzenbach, and S. W. Chisholm. 1993. Simulating bacterial clustering around phytoplankton cells in a turbulent ocean. Limnol. Oceanogr. 38:36–51.

Brown, D. A., and H. C. Berg. 1974. Temporal stimulation of chemotaxis in Escherichia coli. Proc. Nat. Acad. Sci. USA 71:1388–1392.

Cheng, S. Y., S. Heilman, M. Wasserman, S. Archer, M. L. Shuler, and M. Wu. 2007. A hydrogel-based microfluidic device for studies of directed cell migration. Lab Chip 7:763–769.

Dertinger, S. K. W., D. T. Chiu, N. L. Jeon, and G. M. Whitesides. 2001. Generation of gradients having complex shapes using microfluidic networks. Anal. Chem. 73:1240–1246.

Diao, J., and others. 2006. A three-channel microfluidic device for generating static linear gradients and its application to the quantitative analysis of bacterial chemotaxis. Lab Chip 6:381–388.

DiLuzio, W. R., L. Turner, M. Mayer, P. Garstecki, D. B. Weibel, H. C. Berg, and G. M. Whitesides. 2005. *Escherichia coli* swim on the right-hand side. Nature 435:12771–12774.

D'Orsogna, M. R., M. A. Suchard, and T. Chou. 2003. Interplay of chemotaxis and chemokinesis mechanisms in bacterial dynamics. Phys. Rev. E 68:021925.

Eisenbach, M. 1999. Sperm chemotaxis. Rev. of Reproduction 4:56–66.

———. 2004. Chemotaxis. Imperial College Press.

Fenchel, T. 2002. Microbial behaviour in a heterogenous world. Science 296:1068–1071.

———. 2003. Biogeography for bacteria. Science 301:925–926.

———, and N. Blackburn. 1999. Motile chemosensory behaviour of phagotrophic protists: Mechanisms for and efficiency in congregating at food patches. Protist 150:325–336.

Ford, R. M., and D. A. Lauffenburger. 1991. Measurement of bacterial random motility and chemotaxis coefficients: II. Application of single-cell-based mathematical model. Biotech. Bioengin. 37:661–672.

———, B. R. Phillips, J. A. Quinn, and D. A. Lauffenburger. 1991. Measurement of bacterial random motility and chemotaxis coefficients: I. Stopped-flow diffusion chamber assay. Biotech. Bioengin. 37:647–660.

Frymier, P. D., R. M. Ford, H. C. Berg, and P. T. Cummings. 1995. 3-Dimensional tracking of motile bacteria near a solid planar surface. Proc. Nat. Acad. Sci. USA 92:6195–6199.

Govoronova, E. G., and O. A. Sineshchekov. 2005. Chemotaxis in the green flagellate alga *Chlamydomonas*. Biochemistry 70:717–725.

Guillard, R. R. L., and J. H. Ryther. 1962. Studies of marine planktonic diatoms. I. Cyclotella nana Hustedt and Detonula confervacea Cleve. Canadian J. Microbiol. 8:229–239.

Hill, J., O. Kalkanci, J. L. McMurry, and H. Koser. 2007. Hydrodynamic surface interactions enable Escherichia coli to seek efficient routes to swim upstream. Phys. Rev. Lett. 98:068101.

Hirota, N., and Y. Imae. 1983. Na^+ driven flagellar motors of an *alkophilic bacillus* strain YN-1. J. Biol. Chem. 258:10577–10581.

Jackson, G. A. 1980. Phytoplankton growth and zooplankton grazing in oligotrophic oceans. Nature 284:439–441

———. 1987. Simulating chemosensory responses of marine microorganisms. Limnol. Oceanogr. 32:1253–1266.

———. 1989. Simulation of bacterial attraction and adhesion to falling particles in an aquatic environment. Limnol. Oceanogr. 34:514–530

Jeon, N. L., S. K. W. Dertinger, D. T. Chiu, I. S. Choi, A. D. Stroock, and G. M. Whitesides. 2000. Generation of solution and surface gradients using microfluidic systems. Langmuir 16:8311–8316.

Keymer, J. E., P. Galajda, C. Muldoon, S. Park, and R. H. Austin. 2006. Bacterial metapopulations in nanofabricated landscapes. Proc. Nat. Acad. Sci. USA 103:17290–17295.

Kiørboe, T., and G. A. Jackson. 2001. Marine snow, organic solute plumes, and optimal chemosensory behaviour of bacteria. Limnol. Oceanogr. 46:1309–1318.

Kohidai, L., P. Kovacs, and G. Csaba. 1996. Chemotaxis of the unicellular green alga *Dunaliella salina* and the ciliated *Tetrhymena pyriformis* – Effects of glycine, lysine, and alanine and their oligopeptides. Bioscience Reports 16:467–476.

Korobkova, E., T. Emonet, J.M.G. Vilar, T.S. Shimizu, and P. Cluzel. 2004. From molecular noise to behavioural variability in a single bacterium. Nature 428:574–578

Koyama, S., D. Amari.e., H. A. Solni, M. V. Novotny, and S. C. Jacobsen. 2006. Chemotaxis assays of mouse sperm on microfluidic devices. Anal. Chem. 78:3354–3359.

Lauga, E., W. R. DiLuzio, G. M. Whitesides, H. A. Stone. 2006. Swimming in circles: Motion of bacteria near solid boundaries. Biophys. J. 90:400–412.

Lazier, J. R. N., and K. H. Mann. 1989. Turbulence and the diffusive layers around small organisms. Deep Sea Res. 36:1721–1733.

Lehman, J. T., and D. Scavia. 1982. Microscale nutrient patches produced by zooplankton. Proc. Nat. Acad. Sci. USA 79:5001–5005.

Lewus, P., and R. M. Ford. 2001. Quantification of random motility and chemotaxis bacterial transport coefficients using individual-cell and population-scale assays. Biotech. Bioengin. 75:292–304.

Lin, F., and E. C. Butcher. 2006. T cell chemotaxis in a simple microfluidic device. Lab Chip 6:1462–1469.

Lovely, P. S., and F. W. Dahlquist. 1975. Statistical measures of bacterial motility and chemotaxis. J. Theoret. Biol. 50:477–496.

Macnab, R. M., and D. E. Koshland. 1972. The gradient-sensing mechanism in bacterial chemotaxis. Proc. Nat. Acad. Sci. USA 69:2509–2512.

Malmcrona-Friberg, K., A. Goodman, and S. Kjelleberg. 1990. Chemotactic responses of marine vibrio sp. Strain S14 (CCUG 15956) to low-molecular weight substances under starvation and recovery conditions. Appl. Env. Microbiol. 56:3699–3704.

Manson, M. D., P. Tedesco, H. C. Berg, F. M. Harold, and C. V. D. Drift. 1977. A protonmotive force drives bacterial flagella. Proc. Nat. Acad. Sci. USA 74:3060–3064.

Mao, H., P. S. Crèmer, and M. D. Manson. 2003. A sensitive, versatile microfluidic assay for bacterial chemotaxis. Proc. Nat. Acad. Sci. USA 100:5449–5454.

Marcos, and R. Stocker. 2006. Microorganisms in vortices: a microfluidic setup. Limnol. Oceanogr.: Methods 4:392–398.

McCarthy, J. J., and J. C. Goldman. 1979. Nitrogenous nutrition of marine phytoplankton in nutrient depleted waters. Science 203:670–672.

Mesibov, R., G. W. Ordal, and J. Adler. 1973. The range of attractant concentrations for bacterial chemotaxis and the threshold and size of response over this range. J. Gen. Phys. 62:203–222.

Miller, T. R., K. Hnilicka, A. Dziedzic, P. Desplats, and R. Belas. 2004. Chemotaxis of *Silicibacter* sp. Strain TM1040 toward dinoflagellate products. Appl. Env. Microbiol. 70:4962–4701.

Mitchell, J. G., A. Okubo, and J. A. Fuhrman. 1985. Microzones surrounding phytoplankton form the basis for a stratified marine microbial ecosystem. Nature 316:58–59.

———, L. Pearson, and S. Dillon. 1996. Clustering of marine bacteria in seawater enrichments. Appl. Env. Microbiol. 62:3716–3721.

———, and K. Kogure. 2006. Bacterial motility: links to the environment and a driving force for microbial physics. FEMS Microbiol. Ecol. 55:3–16.

Nachman, G. 2006. A functional response model of a predator population foraging in a patchy habitat. J. Animal Ecol. 75:948–958.

Packer, H. L., and J. P. Armitage. 1994. The chemokinetic and chemotactic behaviour of *Rhodobacter sphaeroides*: Two independent responses. J. Bacteriol. 176:206–212.

Park, S., P. M. Wolanin, E. A. Yuzbahyan, H. Lin, N. C. Darnton, J. B. Stock, P. Silberzan, and R. Austin. 2003. Influence of topology on bacterial social interaction. Proc. Nat. Acad. Sci. USA 100:13910–13915.

Pfeffer, W. 1888. Untersuchungen aus dem Botanischen Institut in Tübingen Ibid 2:582–661.

Quake, S. R., and A. Scherer. 2000. From micro- to nanofabrication with soft materials. Science 290:1536–1540.

Silverman, M. and M. Simon. 1974. Flagellar rotation and the mechanism of bacterial motility. Nature 249:73–74.

Seuront, L., V. Gentilhomme, and Y. Lagadeuc 2002. Small-scale nutrient patchiness in tidally mixed coastal waters. Mar. Ecol. Prog. Ser. 232:29–44

Seymour, J.R., Marcos, and R. Stocker 2008. Resource patch formation and exploitation throughout the marine microbial food web. Am. Nat. In press.

Stocker, R., J. R. Seymour, A. Samadani, D. H. Hunt, and M. Polz. 2008. Rapid chemotactic response enables marine bacteria to exploit ephemeral microscale nutrient patches. Proc. Nat. Acad. Sci. USA 105:4209–4214.

Unger, M. A., H-P. Chou, T. Thorsen, A. Scherer, and S. R. Quake. 2000. Monolithic microfabricated valves and pumps by multilayer soft lithography. Science 288:113–116.

Vicker, M. G. 1981. Ideal and nonideal concentration gradient propagation in chemotaxis studies. Exp. Cell Res. 136:91–100.

Weibel, D. B., W. R. DiLuzio, and G. M. Whitesides. 2007. Microfabrication meets microbiology. Nature Rev.: Microbiol. 5:209–218.

Whitesides, G. M., E. Ostuni, S. Takayama, X. Jiang, and D. E. Ingber. 2001. Soft lithography in biology and biochemistry. Ann. Rev. Biomed. Eng. 3:335–373.

Wu, H., B. Huang, and R. N. Zare. 2006. Generation of complex, static solution gradients in microfluidic channels. J. Am. Chem. Soc. 128:4194–4195.

Zhulin, I. B., and J. P. Armitage. 1993. Motility, chemokinesis and methylation-independent chemotaxis in *Azospirillum brasilenese*. J. Bacteriol. 175:952–958.

Submitted 2 March 2008
Revised 13 July 2008
Accepted 4 August 2008